

Population-grating transfer in cold cesium atoms

G. C. Cardoso, V. R. de Carvalho, S. S. Vianna, and J. W. R. Tabosa

Departamento de Física, Universidade Federal de Pernambuco, 50670-901 Recife, PE, Brazil

(Received 23 February 1998)

Optical-pumping-induced population-grating transfer between hyperfine levels of the cesium D_2 line is observed through four-wave mixing in a sample of cold atoms. Diffraction efficiencies of order of 1% have been measured for a large range of angular apertures. We have studied the angular dependence of the diffracted signal in the limit of small atomic velocities and discussed its application for a nondestructive diagnostic of the trap dynamic. Image processing with nearly degenerate frequency conversion was also demonstrated using this specific mechanism. [S1050-2947(99)05302-0]

PACS number(s): 32.80.Pj, 42.50.Hz, 42.65.Hw

Laser-induced dynamic gratings have been studied for the last three decades and is a wide interest field owing to its several possibilities of applications [1]. Of particular importance in these studies is the phenomenon of four-wave mixing (FWM), which can be used as a real time holographic technique to study the processes of writing and reading of a dynamic grating in a nonlinear medium [2]. Among its many applications, the possibility of achieving optical phase conjugation (OPC) and image processing of an optical beam are of special interest and have been demonstrated previously using either photorefractive materials [3], semiconductor doped glasses [4], and organic liquids [5]. FWM has also been performed in atomic vapors [6,7] and the figure of merit of such nonlinear medium evidenced [7]. More recently, several groups have demonstrated a different type of laser-induced dynamic grating [8]. In contrast with the case of FWM in thermal vapors where the atoms are free to move along the grating period, here a three-dimensional (3D) intensity and polarization modulation, associated with a number of interfering laser beams, creates a 3D spatial structure of nearly harmonic potential well, called optical lattice, which can trap and accumulate a considerable fraction of atoms leading to a corresponding spatial structure in the atomic distribution. Bragg light scattering from these optical lattices has recently been reported [9], evidencing a long-range spatial order in this system. On the other hand, the use of cold atoms to perform FWM is also a well-related topic since in this regime the induced population or polarization gratings are basically not affected by the atomic motion (i.e., the time for an atom to move a grating period is much longer than the spontaneous lifetime) and this system can also lead to a long-lived spatial modulation of some local atomic observable, giving rise to a corresponding dynamic atomic grating. This fact also makes cold atoms a very attractive system to perform efficient OPC for large angular aperture of the incident beams [10,11].

In this paper we report on the observation of nearly degenerate four-wave mixing (NDFWM) in cold cesium atoms via optical pumping-induced population-grating transfer between hyperfine levels of cesium D_2 line. This process can lead to the production of a population grating in a long-lived ground state. It is based on a suggestion of Ducloy, de Oliveira, and Bloch [12] of achieving OPC using a pair of

two-level systems, where a grating is created in one pair of levels and read in the other. This is of considerable interest since the dynamics of such a grating can give information about the atomic diffusion in the limit of very low velocities. It has been demonstrated previously by Glassner and Knize [13] that the angular dependence of the FWM signal can be used to measure atomic diffusion in a homogeneously broadened atomic vapor. Although for the typical velocities of laser-cooled atoms, this angular dependence is strongly reduced when the grating decay is determined by the excited state lifetime [2]; Hemmerich, Weidemüller, and Hänsch [14] have demonstrated that FWM performed in a 3D optical lattice can lead to the observation of very narrow resonances whose width is determined by the decay rate of the induced hologram. Besides the possibility of studying similar effects, the process of transferring an induced grating to a weakly interacting ground state also opens a way to perform saturation-free measurements. Furthermore, we demonstrate that the NDFWM signal presents essentially the same properties previously observed in FWM, specifically regarding image processing with frequency conversion and wave-front reconstruction of an object beam.

Our experiment was performed using cold atoms obtained from a vapor cell four-beam magneto-optical trap (MOT) [15]. One pair of molasses beams was added to this scheme to increase the number of trapped atoms. The trapping and molasses beams are provided by a stabilized Ti:sapphire laser and are red detuned by about 12 MHz from the resonance frequency of the cesium cycling transition $6S_{1/2}$, $F=4-6P_{3/2}$, $F'=5$ at $\lambda=852$ nm, as indicated in Fig. 1(a), which shows the hyperfine levels of the cesium D_2 line. The necessary repumping laser is provided by a long external cavity diode laser [16], which is tuned into resonance with the $6S_{1/2}$, $F=3-6P_{3/2}$, $F'=3$ transition. Typically the number of trapped atoms, estimated either by measuring the emitted fluorescence or the absorption of a probe beam by the atomic cloud is of the order of 10^7 atoms. The experimental geometry to observe the NDFWM signal is depicted in Fig. 1(b). The forward (F) pump and the probe (P) beams (the grating beams) have the same frequency ω_1 and are incident in the trap forming an angle of $\theta \approx 4^\circ$. These beams are provided by a grating-stabilized diode laser. Another independent, grating-stabilized diode laser, generates the back-

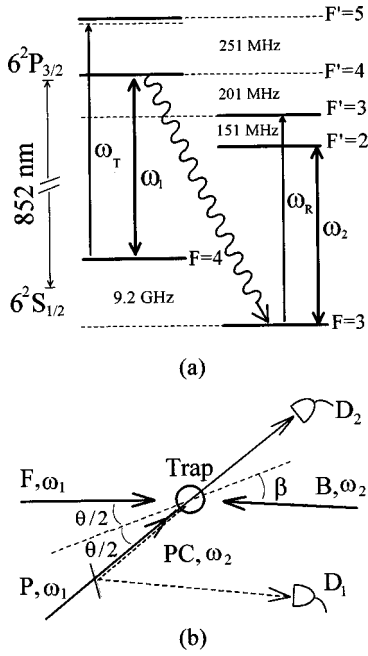


FIG. 1. (a) Hyperfine energy levels of cesium D_2 line. The arrows indicate the laser frequencies interacting with the corresponding transitions. (b) Experimental beam arrangement for observing the NDFWM signal. The forward (F) and the probe (P) beams have the same frequency ω_1 , while the backward (B) beam has frequency ω_2 .

ward (B) pump beam (the diffracting beam), with frequency ω_2 , and incident on the trap satisfying the phase-matching condition, i.e., $\sin\beta = (\omega_1/\omega_2)\sin\theta/2$. The phase conjugate (PC) beam (the diffracted beam), which is nearly counter-propagating to the probe beam, is picked up from a 50:50 beam splitter and detected directly by a calibrated photodiode. All the FWM beams have approximately the same beam waist of ~ 3 mm, which is much larger than the trap size (~ 2 mm). Figure 2 shows the observed PC spectra, when the frequency ω_2 of the B beam is resonant with the $6S_{1/2}$, $F=3-6P_{3/2}$, $F'=2$ transition, while ω_1 frequency is tuned around the transitions $6S_{1/2}$, $F=4-6P_{3/2}$, $F'=3,4,5$. The spectra are shown for different relative beam polarizations. In Fig. 2(b) all the beams have the same linear polarization and in Fig. 2(c) the polarization of the B beam is orthogonal to that of F and P . However, as shown in Fig. 2(d), when the grating beams F and P have orthogonal polarization states (i.e., either linear or circular states), the diffracted signal is strongly reduced. The spectrum shown in Fig. 2(a) corresponds to the probe (P) absorption spectrum. As indicated in Fig. 2, we only can observe the NDFWM signal when the frequency ω_1 is resonant with a noncycling transition of cesium, in contrast with the case of degenerate four-wave-mixing process previously studied [11]. This indicates that the observed NDFWM signal necessarily involves a process of grating transfer via spontaneous emission from one of the excited states to the lower ground state. The atomic population grating is created by the interference of F and P beams and has a spatial period of $\Lambda = 2\pi/|k_F - k_P| = \lambda/(2\sin\theta/2)$ ($k_{F,P}$ being the corresponding wave vector). The B beam is then diffracted into this grating when its direction of propagation satisfies the Bragg condition. This

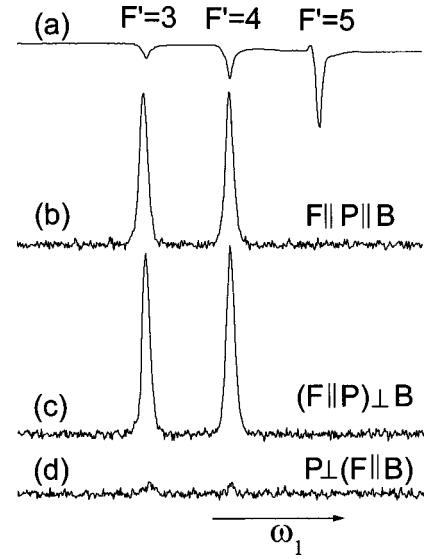


FIG. 2. (a) Probe beam absorption spectra around the transition $6S_{1/2}$, $F=4-6P_{3/2}$, $F'=3,4,5$. (b), (c), and (d) NDFWM spectrum for different relative polarizations of the F , P , and B beams as discussed in the text. For these spectra the B beam frequency ω_2 is resonant with the transition $F=3-F'=2$, while the ω_1 is scanned around the transition $F=4-F'=3,4,5$.

interpretation is also corroborated with the observed polarization dependence. A population grating will only exist for parallel polarization of F and P beams. On the other hand, when these beams have orthogonal polarization, the induced grating will correspond to a Zeeman coherence grating that can only generate a conjugate beam when the diffracting beam is coherently coupled with this induced grating [17]. Since in this NDFWM process there exists a spontaneous emission step, the induced Zeeman coherence is strongly destroyed, leading to a corresponding decrease in the diffraction efficiency. However, as shown in Figs. 2(b) and 2(c), the generated signal is only slightly sensitive to the polarization of the diffracting beam. Moreover, we have checked that the polarization of the generated beam is always the same as that of the diffracting beam. All the spectra presented in Fig. 2 correspond to averaging over eight scans and the observed peaks linewidth are mainly limited by the jitter in the diode laser frequency. The power of the F , P , and B beams is approximately 90, 34, and 100 μW , respectively, in all the spectra shown in Fig. 2. The estimated reflectivity is about 1% as measured relative to the probe beam power. Similar spectra with the same polarization dependence were also observed when the frequency ω_2 was tuned into resonance with the $6S_{1/2}$, $F=3-6P_{3/2}$, $F'=3$ transition. However, in this case one of the peaks will have, in addition to the contribution coming from the transferred grating, a coherent resonant contribution associated with a nonlinear polarization induced by the three incident beams in the $F=4-F'=3-F=3$ three level system. In fact, this process offers the possibility to investigate the interference between the fields generated via a two- and a three-level atomic system.

In modeling our system we have performed a density matrix calculation using the four hyperfine levels that interact directly with the FWM beams as well as the levels coupled with the trapping and the repumping beams. We have accounted for the effect of the trapping and the repumping

lasers through incoherent optical pumping rates specified by γ_T and γ_R , respectively. For the specific situation depicted in Fig. 1(a), we take the incident electromagnetic fields to be of the form $\vec{E}_\mu = \frac{1}{2} \vec{A}_\mu e^{i(\omega_\mu t - \vec{k}_\mu \cdot \vec{r})} + \text{c.c.}$, with $\mu = F, P, B$, $\omega_F = \omega_P = \omega_1$, $\omega_B = \omega_2$, and with A_μ being the complex field amplitude. We assume a single relaxation rate γ for all the excited states. The populations of the states $F' = 4$, $F' = 2$, $F = 4$, and $F = 3$, i.e., $\sigma_{4'4'}^{(2)}$, $\sigma_{2'2'}^{(2)}$, $\sigma_{44}^{(2)}$, and $\sigma_{33}^{(2)}$ are calculated up to second order in the fields F and P and act as source terms to determine the third-order non-

linear optical coherence $\rho_{32'}^{(3)} = \sigma_{32'}^{(3)} e^{i[\omega_B t - (\vec{k}_F - \vec{k}_P + \vec{k}_B) \cdot \vec{r}]}$. A straightforward perturbative density matrix calculation in the rotating-wave approximation, yields for the on-resonance coherence amplitude the following result:

$$\sigma_{32'}^{(3)} = \frac{i}{2} \frac{\mu_{32'} A_B}{\hbar} \frac{(\sigma_{2'2'}^{(2)} - \sigma_{33}^{(2)})}{[\gamma/2 - i(\vec{k}_F - \vec{k}_P + \vec{k}_B) \cdot \vec{v}]}, \quad (1)$$

with

$$\begin{aligned} \sigma_{2'2'}^{(2)} - \sigma_{33}^{(2)} = & -\frac{N}{4} \left(\frac{\gamma_T + \gamma}{2\gamma_T + \gamma} \right) \left(\frac{1}{\gamma/2 - i\vec{k}_F \cdot \vec{v}} + \frac{1}{\gamma/2 + i\vec{k}_P \cdot \vec{v}} \right) \\ & \times \frac{|\mu_{44'}|^2 A_F A_P^*}{\hbar^2} \frac{\gamma(\gamma_R + \gamma + \delta_v)}{[4\delta_v^2(\gamma + \gamma_R + \delta_v/2) + \gamma^2(\gamma_R + 2\delta_v + 5\gamma_R\delta_v/\gamma)]} \end{aligned}$$

and $\delta_v = -i(\vec{k}_F - \vec{k}_P) \cdot \vec{v}$. In the above expression $\mu_{44'}$ and $\mu_{32'}$ are the dipole matrix elements for the considered transitions, N is the total number of atoms in the trap, and \vec{v} is the atomic velocity. This induced polarization will generate a field with frequency ω_2 and propagating along the direction $\vec{k}_{PC} = \vec{k}_F + \vec{k}_B - \vec{k}_P$, when the phase-matching condition discussed previously is satisfied.

As it can be seen from Eq. (1), the effect of the trapping laser, which is nearly resonant with the closed transition $F=4-F'=5$, only corresponds to an overall multiplicative factor in the field amplitude. We are neglecting the off-resonance trapping laser excitation to the level $F'=4$, which is much smaller than the optical pumping rate induced by the resonant wave-mixing beams. However, the repumping laser plays a more fundamental role in determining the amplitude of the observed signal. In order to analyze this point, we have numerically integrated Eq. (1) over the range of atomic velocities usually present in the trap. We have assumed a Maxwell-Boltzmann velocity distribution with a rms thermal velocity u . The observed signal intensity is proportional to $|\langle \sigma_{32'}^{(3)} \rangle|^2$, where $\langle \sigma_{32'}^{(3)} \rangle$ is the velocity-averaged coherence amplitude. The results, shown in Fig. 3, represent the angular dependence of the relative NDFWM signal intensity, for different values of the repumping rate γ_R . We have assumed that the Doppler width (ku) associated with the velocity distributions is two orders of magnitude smaller than the spontaneous emission rate γ . According to Fig. 3, for $\gamma_R \leq ku \ll \gamma$, we predict an angular dependence for the generated signal. This is very different from the calculated, very small angular dependence of the FWM signal for a closed two-level system in the limit of very small velocities associated with laser-cooled atoms. In the last case, the time for an atom to move a grating period is much longer than the excited state lifetime ($\sim \gamma^{-1}$), so the washing out of the grating due to the atomic motion is strongly reduced [2]. However, for the specific grating transfer mechanism considered here, the washout of the transferred population grating will be deter-

mined both by the atomic motion and by the optical repumping rate γ_R , which determines the effective lifetime of the lower ground state. Therefore, for very small values of γ_R , the effect of the atomic motion can be evidenced. This opens the perspective to employ the grating transfer mechanism to perform a nondestructive diagnostic of the trap dynamics, where the measurement of the angular dependence of the diffracted signal would provide direct information of the average atomic velocity perpendicular to the grating planes.

In fact, we have measured the angular dependence of the diffracted signal and the results are presented in Fig. 4. Although we believe that this observed angular dependence is directly associated with the atomic motion, if we attempt to fit these data with the present theoretical model, we achieve only a qualitative agreement. That is, for the experimental estimated range of repumping rate, we obtain an atomic av-

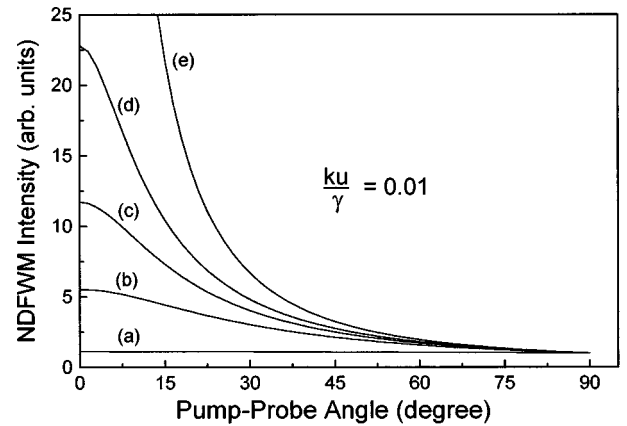


FIG. 3. Relative NDFWM intensity as a function of the angle between the grating beams, F and P , for different values of the optical repumping rate discussed in the text. (a) $\gamma_R/\gamma = 10^{-1}$, (b) $\gamma_R/\gamma = 10^{-2}$, (c) $\gamma_R/\gamma = 6 \times 10^{-3}$, (d) $\gamma_R/\gamma = 4 \times 10^{-3}$, and (e) $\gamma_R/\gamma = 10^{-3}$. The vertical scale for each curve is normalized by the signal intensity at $\theta=90^\circ$. For curve (e), the ratio between the signal at $\theta=0$ and $\theta=90^\circ$ is 290.

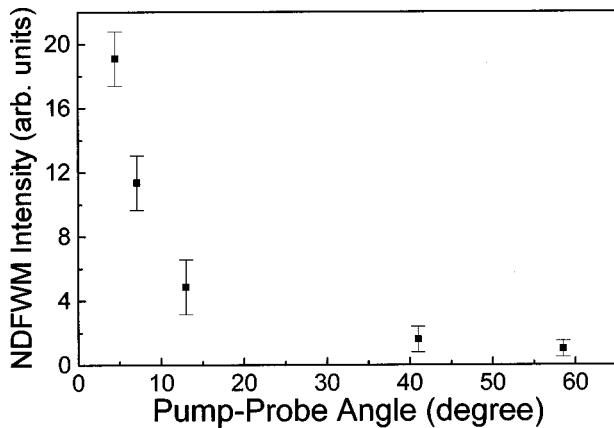


FIG. 4. Angular dependence for the NDFWM signal. The frequencies ω_1 and ω_2 are resonant with the transitions $F=4-F'=4$ and $F=3-F'=2$, respectively. For these data the molasses beams were replaced by MOT beams in order to get a symmetric cloud in the transverse plane.

erage velocity, which is systematically larger than the average velocity estimated by performing a time-of-flight measurement. We attribute this discrepancy to the fact that for the data presented in Fig. 4, the FWM beams intensities are much higher than the saturation intensity, where the above perturbative model can no longer be employed.

Turning now to a different aspect of this problem, we have, according to Eq. (1), that the complex field amplitude of the generated signal is proportional to the complex conjugate of the probe field amplitude. As it is well known, this can lead to the observation of real-time optical image processing and wave-front rectification [1,2]. Actually we have demonstrated both effects. We have been able to demonstrate that the process under investigation can be used to transfer an image impressed onto the probe beam wave front (a fringe pattern), oscillating at a frequency ω_1 to the diffracted signal beam, oscillating with different frequency ω_2 [18]. Although, as we have mentioned, similar demonstrations have been performed previously [3,5], we emphasize that in our system the temporal response is determined by the optical pumping time, which can be much shorter than that of photorefractive materials. Furthermore, we have also demonstrated that our system can perform wave-front reconstruc-

tion by placing an aberrator (a transparent Scotch tape glued into a glass plate) in the way of the probe beam and observing that the aberrations impressed onto the probe beam wave front were corrected after the diffracted signal beam has traveled back through the same aberrator. Although the phase-matching condition imposes that the diffracted signal beam does not exactly counterpropagate with the probe beam, the misalignment is very small and lies in the range of $\sim \mu\text{rad}$. It is worth mentioning that these effects can be achieved for a large range of angular apertures between the ‘‘object’’ probe (P) beam and the forward (F) pump beam. In fact, according to Fig. 4, we have been able to efficiently observe NDFWM for an aperture angle as high as $\theta \approx 60^\circ$. This is in great contrast with the strong angular dependence of the OPC signal in thermal atomic vapors [19], which represents a major drawback for this kind of application.

In conclusion, we have observed FWM-induced population-grating transfer between hyperfine levels of cold cesium atoms. We have theoretically studied the angular dependence of the NDFWM signal in the range of small atomic velocities and suggested that this grating transference process can be used as an alternative nondestructive tool to diagnose the trap dynamics. We have also demonstrated that this process can lead to image processing of an optical signal with frequency conversion and with a time response determined by the optical pumping time. Moreover, the observed signal has been used to perform wave-front rectification and since its efficiency is weakly dependent of the angular aperture, this process can add new perspectives in the application of OPC as a real time holographic process.

Another technique, which can also provide direct information on the velocity distribution of the cold sample, consists in measuring the grating decay time when the grating beams are switched off. We are currently investigating this process [20]. It is worth mentioning that these techniques can monitor the atomic average velocity along an arbitrary direction.

We are very grateful to Professor J. R. Rios Leite and Professor G. Grynberg for stimulating discussions. This work was supported by the following Brazilian Agencies: Financiadora de Estudos e Projetos (FINEP), Conselho Nacional de Desenvolvimento Científico e Tecnológico, CNPq e Fundação de Amparo à Ciência e Tecnologia de Pernambuco, FACEPE.

[1] H. J. Eichler, P. Lünter, and D. W. Pohl, *Laser Induced Dynamic Gratings* (Springer-Verlag, New York, 1985).
 [2] Robert A. Fisher, *Optical Phase Conjugation* (Academic, New York, 1983); M. Gower and D. Proch, *Optical Phase Conjugation* (Springer-Verlag, New York, 1994), pp. 97–119.
 [3] Jeffrey O. White and Amnon Yariv, *Appl. Phys. Lett.* **37**, 5 (1980).
 [4] R. K. Jain and R. C. Lind, *J. Opt. Soc. Am.* **73**, 647 (1983).
 [5] C. Martin and R. W. Hellwarth, *Appl. Phys. Lett.* **34**, 371 (1979).
 [6] P. F. Liao, D. M. Bloom, and N. P. Economou, *Appl. Phys. Lett.* **32**, 813 (1978); L. M. Humphrey, J. P. Gordon, and P. F.

Liao, *Opt. Lett.* **5**, 56 (1980); M. Oriá, D. Bloch, M. Fichet, and M. Ducloy, *ibid.* **14**, 1082 (1989).
 [7] B. Ai, D. S. Glassner, R. J. Knize, and J. P. Partanen, *Appl. Phys. Lett.* **64**, 951 (1994).
 [8] C. I. Westbrook, R. N. Watts, C. E. Tanner, S. L. Ralston, W. D. Phillips, P. D. Lett, and P. L. Gould, *Phys. Rev. Lett.* **65**, 33 (1990); N. Bigelow and M. Prentiss, *ibid.* **65**, 29 (1990); G. Grynberg, B. Lounis, P. Verkerk, J.-Y. Courtois, and C. Salomon, *ibid.* **70**, 2249 (1993); A. Hemmerich, C. Zimmermann, and T. Hänsch, *ibid.* **22**, 89 (1993).
 [9] G. Birkl, M. Gatzke, I. H. Deutsch, S. L. Rolston, and W. D. Phillips, *Phys. Rev. Lett.* **75**, 2823 (1995); M. Weidemüller, A.

- Hemmerich, A. Görlitz, T. Esslinger, and T. W. Hänsch, *ibid.* **75**, 4583 (1995).
- [10] L. Hilico, P. Verkerk, and G. Grynberg, *C. R. Acad. Sci. (Paris)* **315**, 285 (1992).
- [11] J. W. R. Tabosa, S. S. Vianna, and F. A. M. de Oliveira, *Phys. Rev. A* **55**, 2968 (1997); J. W. R. Tabosa and S. S. Vianna, *Braz. J. Phys.* **27**, 243 (1997).
- [12] M. Ducloy, F. A. M. de Oliveira, and D. Bloch, *Phys. Rev. A* **32**, 1614 (1985).
- [13] D. S. Glassner and R. J. Knize, *Phys. Rev. Lett.* **74**, 2212 (1995).
- [14] A. Hemmerich, M. Weidemüller, and T. Hänsch, *Europhys. Lett.* **27**, 427 (1994).
- [15] C. Chesman, E. G. Lima, F. A. M. de Oliveira, S. S. Vianna, and J. W. R. Tabosa, *Opt. Lett.* **19**, 1237 (1994); J. W. R. Tabosa, S. S. Vianna, and C. A. Benevides, *Opt. Commun.* **116**, 77 (1995).
- [16] L. Viana, S. S. Vianna, M. Oriá, and J. W. R. Tabosa, *Appl. Opt.* **35**, 368 (1996).
- [17] S. Le Boiteux, P. Simoneau, D. Bloch, F. A. M. de Oliveira, and M. Ducloy, *IEEE J. Quantum Electron.* **QE-22**, 1229 (1986).
- [18] G. C. Cardoso, V. R. de Carvalho, S. S. Vianna, and J. W. R. Tabosa (unpublished).
- [19] M. Ducloy and D. Bloch, *J. Phys. (Paris), Colloq.* **42**, 711 (1981); C. L. César, J. W. R. Tabosa, P. C. de Oliveira, M. Ducloy, and J. R. Rios Leite, *Opt. Lett.* **13**, 1108 (1988).
- [20] A. Lezama, G. C. Cardoso, S. S. Vianna, and J. W. R. Tabosa (unpublished).